

## Probabilistic Seismic Risk Assessment

### 1. Probabilistic Seismic Hazard Analysis (PSHA)

The hazard curve is based on location-specific ground motion and was derived from a catalogue of 500,000 years during which 100,224 simulated events were considered. The source parameters used are listed in figure 1.

**Figure 1: Source Parameters Set by the Task**

Source Parameter	Source Parameter Value
$\lambda$	0.2
$m_{max}$	4.5
$m_{min}$	7
$R_{jb}$ of building A	17
$R_{jb}$ of building B	10
b-value	1

The inter-arrival time  $t$  is determined (Otárola 2023) and visualized (see figures 2 and 3):

$$t = \frac{-\ln(1-u)}{\lambda}$$

where  $u$  is a uniformly distributed random number.

**Figure 2: Inter-arrival Time – PDF**

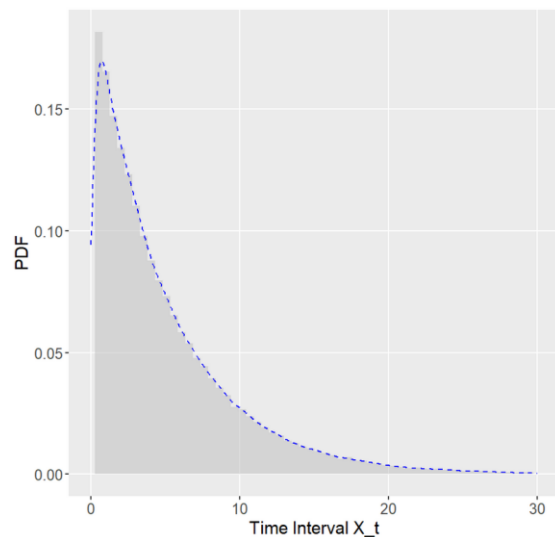
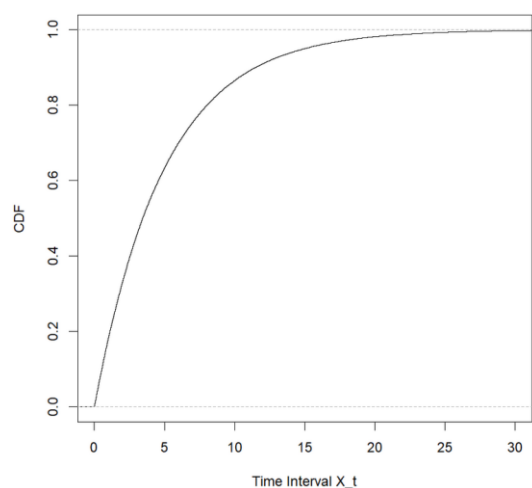


**Figure 3: Inter-arrival Time – CDF**



Magnitudes are simulated (Otárola 2023) and visualized (see figure 4 and 5):

$$m = \frac{\log(1-u) \times (1 - 10^{-b(m_{max}-m_{min})})}{b} + m_{min}$$

where  $u$  is a uniformly distributed random number.

**Figure 4: Magnitude Simulation – PDF**

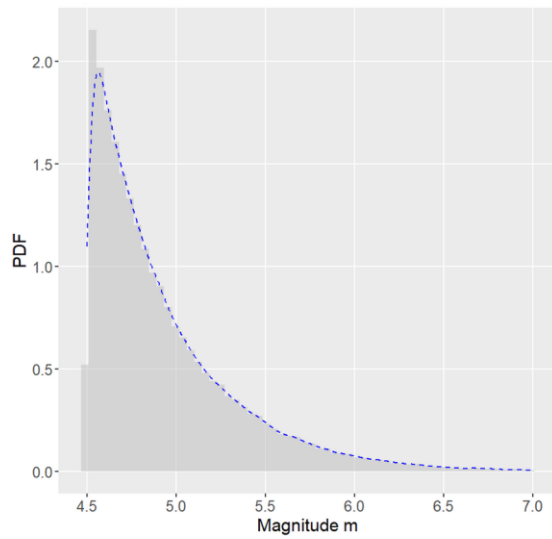
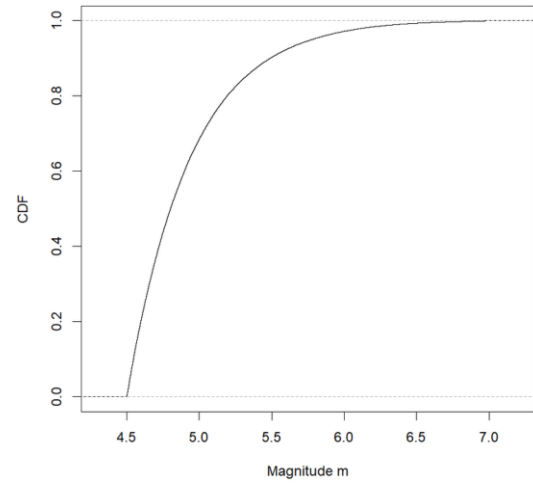


**Figure 5: Magnitude Simulation – CDF**



To simulate ground motion intensity, a formula which accounts for constant geophysical properties is adapted from Akker and Bommer (2010). Here, it disregards terms that equal to zero:

$$\log_{10}(PGA) = b_1 + b_2m + b_3m^2 + (b_4 + b_5m)\log\sqrt{R_{jb}^2 + b_6^2} + \varepsilon\sqrt{\sigma_1^2\sigma_2^2}$$

with parameters assuming the values shown in figure 6. Since  $\varepsilon \sim N(0,1)$ , it scales the standard deviations and accounts for aleatory uncertainty.

**Figure 6: Ground Motion Intensity Parameters at T=0.00 (Akker and Bommer (2010))**

Parameter	Parameter Value
b1	1.04159
b2	0.91333
b3	- 0.08140
b4	- 2.92728
b5	0.28120
b6	7.86638
$\sigma_1$	0.2610
$\sigma_2$	0.0994

Then,  $\log_{10}(PGA)$  is converted to PGA which is subsequently converted from  $\text{cm/s}^2$  to g (Convertunits 2023). The simulation's distributions are displayed in figure 7 and 8.

**Figure 7: Ground Motion Intensity Measure Sampling**

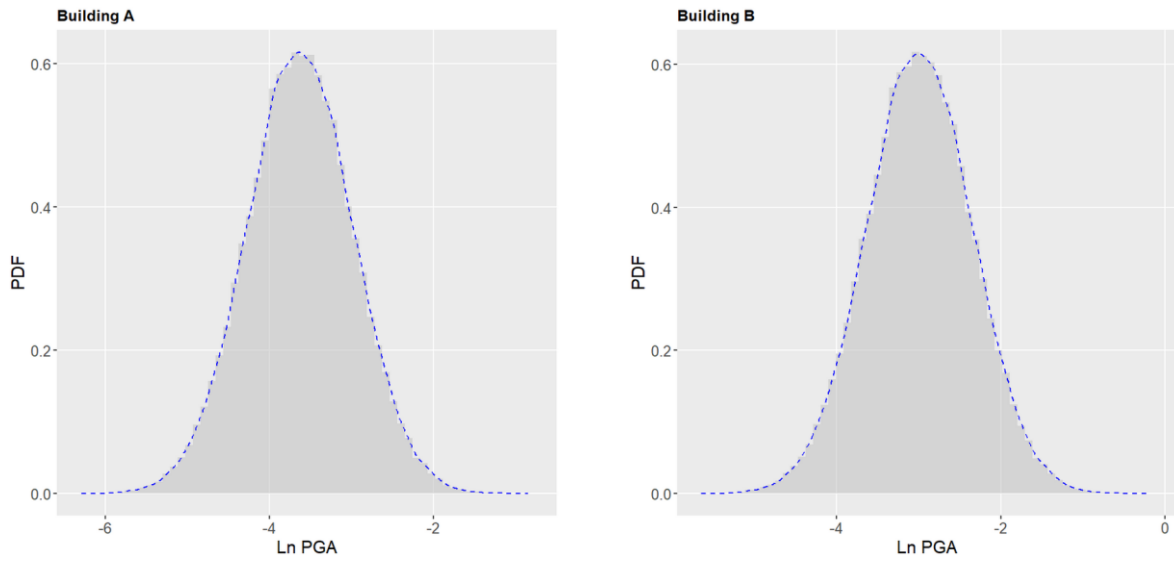
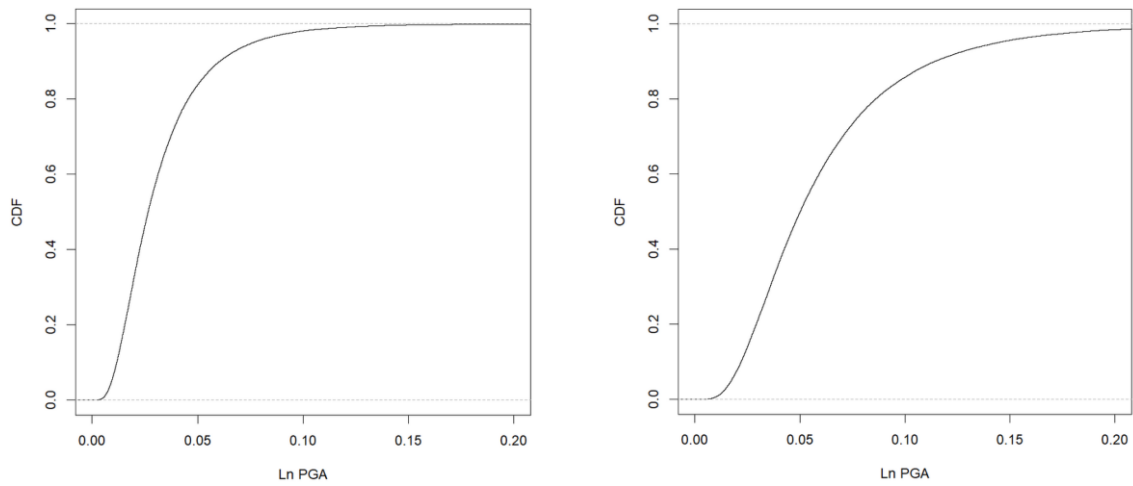


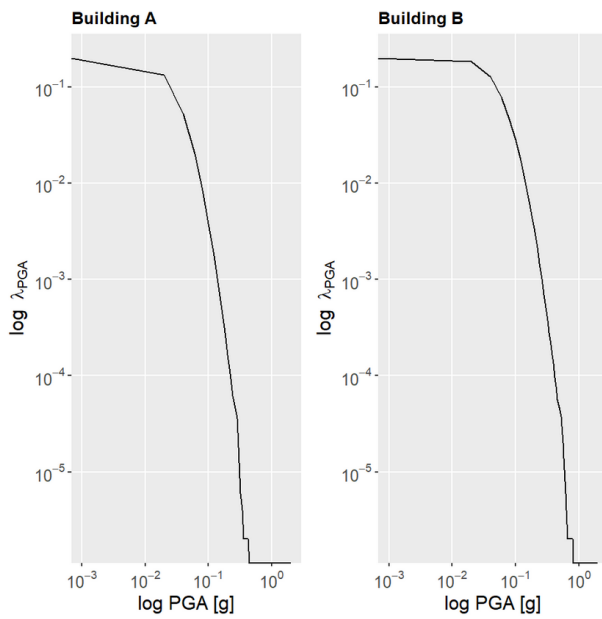
**Figure 8: Ground Motion Intensity Measure Sampling – CDF**



Finally, hazard curves (see figure 9) are created. They display the number of PGAs exceeding a set of intensity measure (IM) levels (Baker 2015; Iacopetti 2023):

$$Pr(IM > x) = \int_{m_{min}}^{m_{max}} Pr(IM > x|m, r) f_M(m) dm$$

**Figure 9: Annual Rate of Exceedance**



## 2. Fragility Curves

Fragility curves translate earthquake intensity into the risk of physical damage, in this case damage of the buildings A and B. The probabilities of reaching or exceeding a damage state  $ds_i$  for a given level of IM are expressed by a standard log-normal cumulative distribution function (Gentile 2023):

$$P(DS \geq ds_i | IM) = \Phi \left( \frac{\ln \left( \frac{IM}{\lambda_{DS}} \right)}{\beta} \right)$$

$\lambda_{DS}$  is “based on median values of spectral displacement of the damage state of interest and an assumed demand spectrum shape that relates spectral response to PGA” (FEMA, 2020, p. 5-55).  $\beta$  is the log-normal standard deviation which is based on uncertainty in the damage state threshold of the structural system and the variability in response due to the spatial variability of ground motion demand (FEMA 2020). The values shown in figure 10 are used in the computation.

**Figure 10: HAZUS fragility curves for reinforced concrete moment resisting frames. Units: median [g]; dispersion [-] (FEMA 2020)**

Building	Height	Code	Equivalent-PGA Structural Fragility							
			Slight		Moderate		Extensive		Complete	
			$\lambda_{DS}$	$\beta$	$\lambda_{DS}$	$\beta$	$\lambda_{DS}$	$\beta$	$\lambda_{DS}$	$\beta$
A	Low-Rise	High Code	0.24	0.64	0.35	0.64	0.7	0.64	1.37	0.64
B	Low-Rise	Pre Code	0.1	0.64	0.12	0.64	0.21	0.64	0.41	0.64

The buildings A and B are between 1 and three stories and around 20 feet high (FEMA 2020). They have frames of reinforced concrete and beams. The damage state definitions can be found in FEMA (2020, p. 5-15).

The fragility curves are shown in figure 11 and 12.

**Figure 11: Fragility Curve for Four Damage States, Building A**

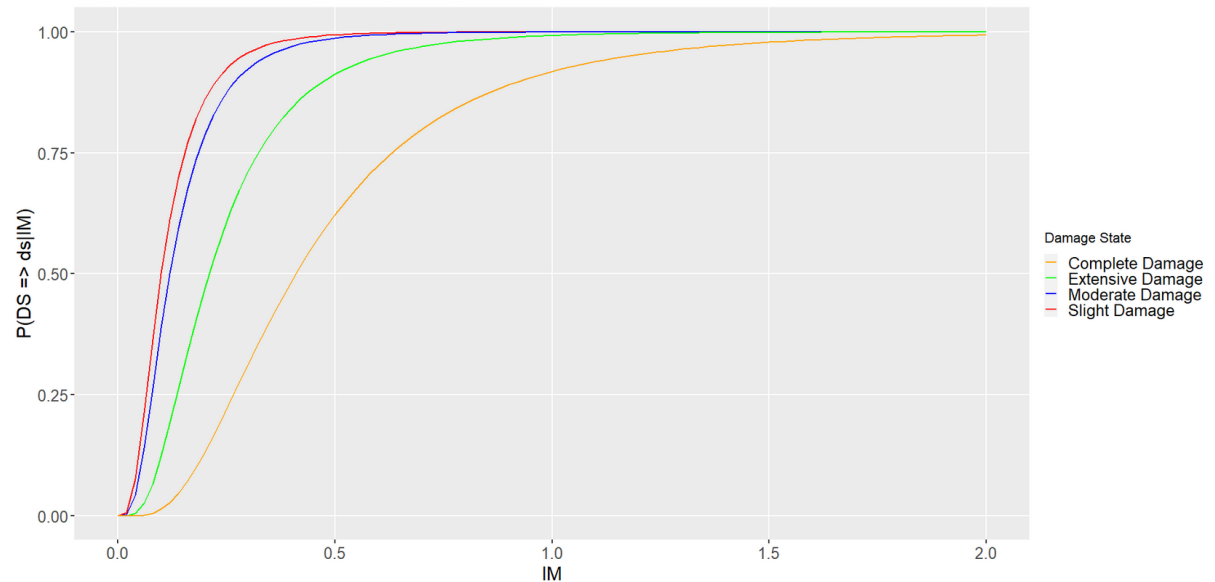
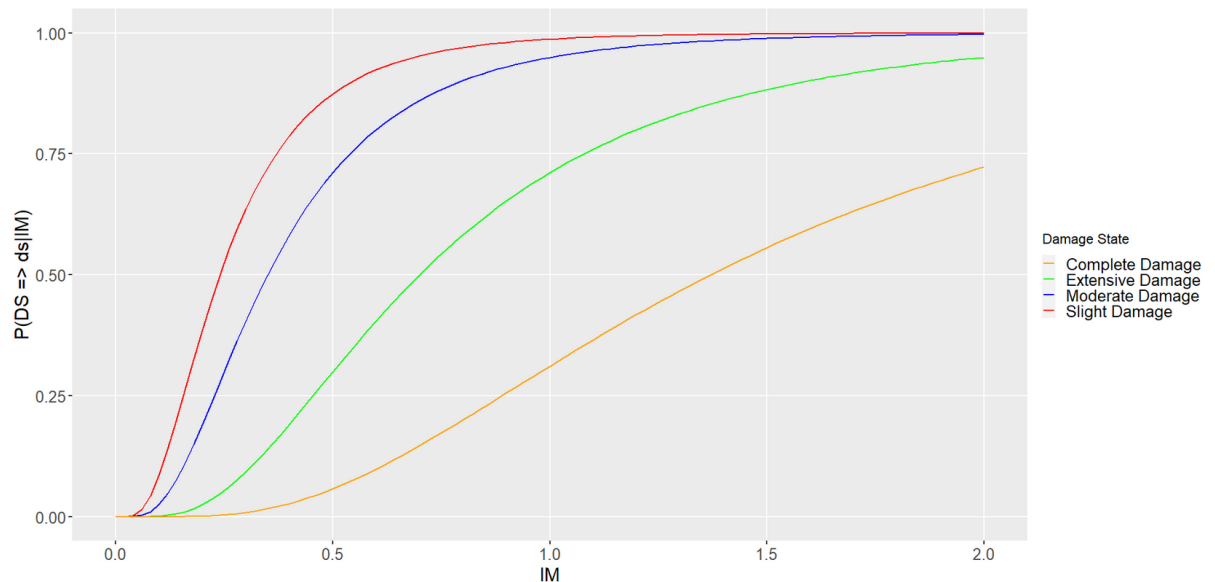


**Figure 12: Fragility Curve for Four Damage States, Building B**



### 3. Loss Curves

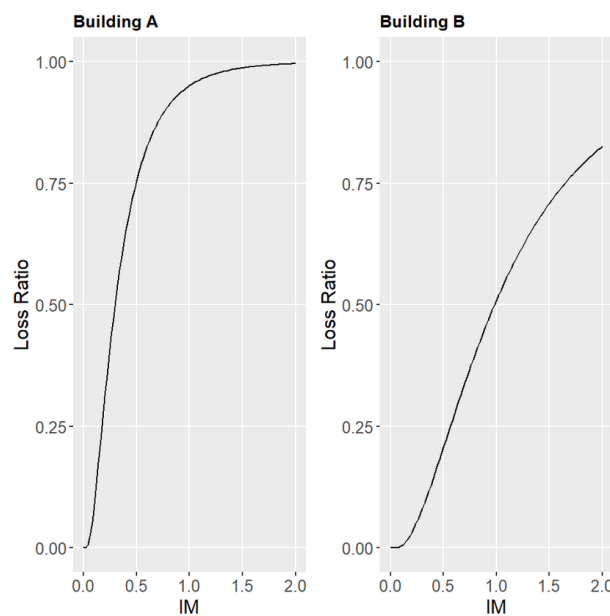
Loss curves translate fragility into financial loss and hence are an important risk analysis tool for stakeholders like home owners and insurances.

The asset-level vulnerability curve maps PGAs and loss ratio for each level of IM. The formula is (Gentile 2023):

$$LR(IM) = \sum_{i=1}^{DS} (F_{DS_{i-1}}(IM) - F_{DS_i}(IM)) DLR_i$$

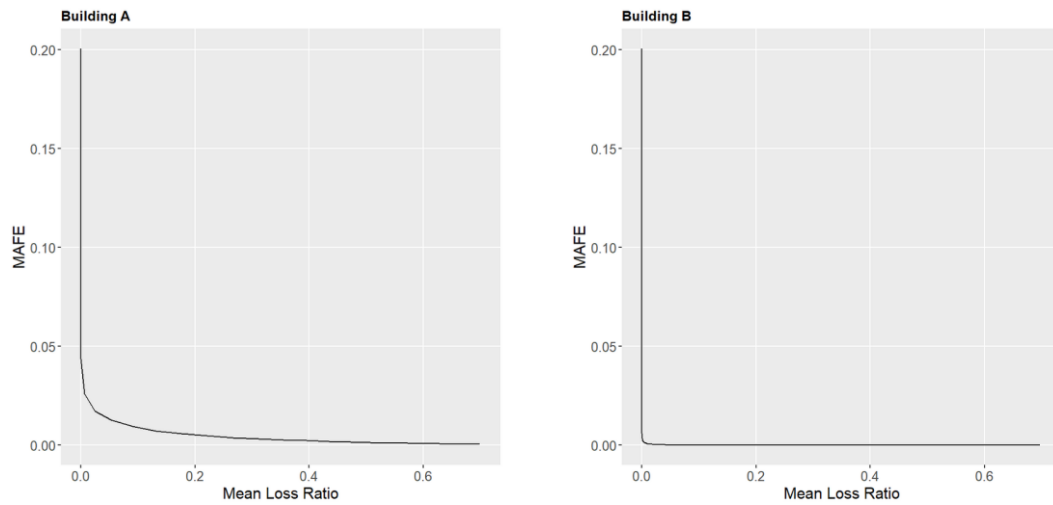
where the damage state-specific DLR are the damage-to-loss-ratio, hence the mean ratio of the repair cost to the total replacement cost. The DLRs set by the task are 2%, 10%, 43.5% and 100% for the four damage states (from slight to complete damage), respectively. This results in vulnerability curves shown in figure 13.

**Figure 13: Vulnerability Curve**



The loss curves (see figure 14) show the mean annual frequency of exceeding (MAFE) the mean loss ratio computed in the vulnerability curve. The corresponding code linearly interpolates mean loss ratio with respect to IM at the points specified by the PGA values and then sums all interpolated losses that exceed the respective level of loss. The accuracy of using interpolation for making predictions and drawing inferences is generally low, in this case especially since I did not explore other interpolation techniques to determine if linear interpolation is the most appropriate method.

**Figure 14: Loss Curves**

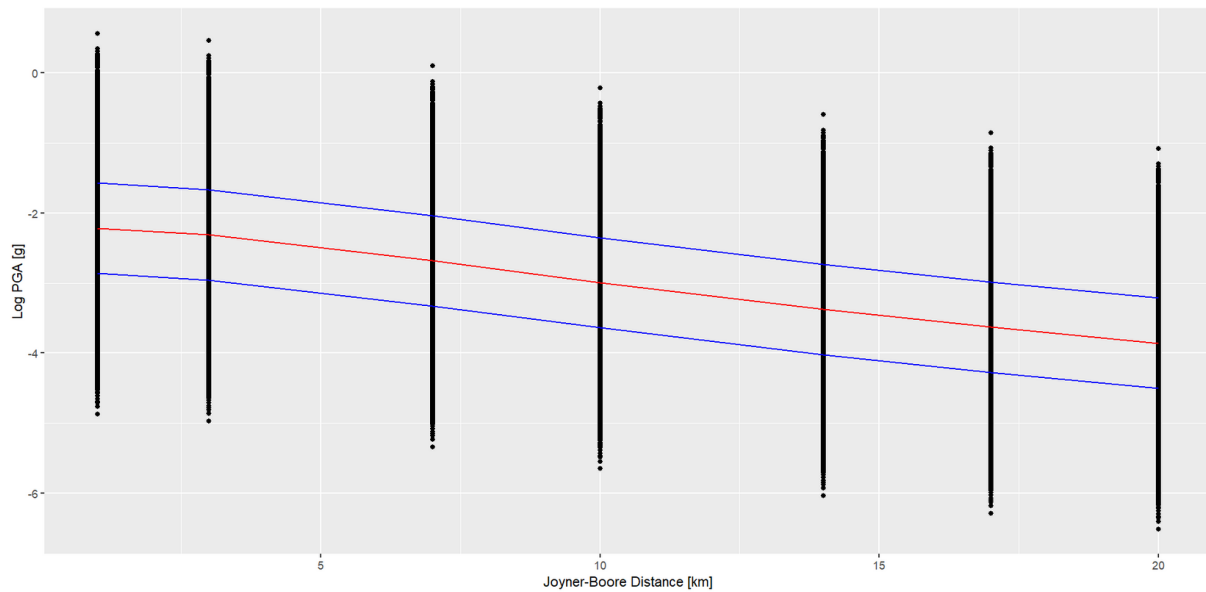


#### 4. Discussion of Results

The PSHA acknowledges uncertainties of deterministic approaches (Baker 2015). It assumes that the events independently follow a Poisson distribution. The inter-arrival times follow an exponential distribution. The decay in figure 1 implies that the likelihood of another earthquake occurring is high soon after and low after more time has passed. The ground motion sampling assumes independent magnitudes (Baker 2015; Iacoletti 2023). As imposed by the formula, the PDFs (logarithmic version see figure 7) are normally distributed.

I conducted an investigation into the variability of simulated ground motion intensity (see figure 14). I use the same formula as in chapter 1, but vary the distances to 1km, 3km, 7km, 14km, and 20km. Since all PDFs follow a normal distribution, not only the likelihood of surpassing the mean (red line) and standard deviations above and below the mean (blue lines), but also of surpassing any other value of PGA reduces as distance increases. This trend aligns with empirical observations (Iacoletti 2023).

**Figure 14: Ground Motion Intensity Measure Sampling Across Space**



The hazard curve formula is adapted from Iacopetti (2023), however, it leaves out the integral over the constant distance. The resulting annual rates of exceedance (see figure 9) decrease quickly, in the mid-range in a nearly linear manner. Even though the differences are small, building B shows slightly higher exceedance probabilities for most levels of IM. This is because it is closer to the fault.

When comparing the fragility curves (see figures 11 and 12), the comparatively steep curve with little distance to each other of building A is noteworthy. This implies that building A is more fragile in a sense that for the same level of IM, it has a higher exceedance probability in all damage states (except for  $IM > 1$  and  $P(DS \geq ds_i | IM)$  close to 1 of the slight and moderate damage state).

By applying the same DLRs, the vulnerability curves (see figure 13) translate the comparatively high fragility of building A into a comparatively high vulnerability for the same level of IM. In contrast, building B does not have a weighted average loss of 100% for any level of IM.

The loss curves (see figure 14) both show  $MAFE = 0.200448$  at mean loss ratio = 0. Then, MAFE approaches 0 rapidly as the mean loss ratio increases. This trend is more extreme for building B than for building A. The strikingly low values might root in an error in the code or weaknesses in the interpolation.



## **Bibliography**

Akker, S. and Bommer, J. (2010): Empirical Equations for the Prediction of PGA, PGV, and Spectral Accelerations in Europe, the Mediterranean Region, and the Middle East, *Seismology Research Letters*, Vol. 81, No. 2, pp. 195-206, doi: 10.1785/gssrl.81.2.195.

Baker, J. (2015): Introduction to Probabilistic Seismic Hazard Analysis, White Paper Version 2.1.

Convertunits (2023): Convert cm/s<sup>2</sup> to g-unit. Conversion of Measurement Units, URL: <https://www.convertunits.com/from/cm/s%5E2/to/g-unit> [accessed on 19th April 2023].

FEMA (2020): Hazus Earthquake Model Technical Manual, Hazus 4.2 SP3.

Gentile, R. (2023): Statistics and Probability for CAT Modelling, Lecture in IRDR008 Catastrophe Modelling, Second Term of Academic Year 2023, University College London.

Iacoletti, S. (2023): Probabilistic Seismic Hazard Analysis (PSHA), Guest Lecture in IRDR008 Catastrophe Modelling, Second Term of Academic Year 2023, University College London.

Otárola, K. (2023): Simulation-based PSHA, Guest Lecture in IRDR008 Catastrophe Modelling, Second Term of Academic Year 2023, University College London.